

## **Crystal growth and characterization of undoped and Dy-doped $\text{TlPb}_2\text{Br}_5$ for Infrared Lasers and Nuclear Radiation Detection**

U. Hömmerich\*, E. Brown, A. Kabir, D. Hart  
Department of Physics, Hampton University, Hampton, Virginia 23668

S. B Trivedi, F. Jin, H. Chen  
Brimrose Corporation of America, 19 Loveton Circle, Baltimore, Maryland 21152

### Abstract

We report results of the crystal growth and characterization of undoped and Dy-doped  $\text{TlPb}_2\text{Br}_5$  for applications in infrared (IR) lasers and nuclear radiation detection.  $\text{TlPb}_2\text{Br}_5$  (TPB) was synthesized from commercial starting materials of  $\text{PbBr}_2$  and  $\text{TlBr}$  and further purified through a combination of zone-refinement and directional solidification. For doping experiments, 2 wt% of  $\text{DyBr}_3$  was added to the purified TPB material. Crystal growth of TPB and Dy: TPB was carried out in a two-zone tube furnace by a vertical Bridgman method. Following optical excitation at  $\sim 1.36 \mu\text{m}$ , the Dy: TPB crystal exhibited efficient mid-IR emission bands centered at  $2.8 \mu\text{m}$  and  $4.3 \mu\text{m}$  with room-temperature lifetimes of 9.5 ms and 5.2 ms, respectively. The peak emission cross-sections were determined to be  $\sim 0.8 \times 10^{-20} \text{ cm}^2$  and  $\sim 0.5 \times 10^{-20} \text{ cm}^2$ , respectively, which makes Dy: TPB a promising candidate for mid-IR laser applications. Besides its potential as a solid-state laser host, an undoped TPB crystal was also tested for gamma-ray detection. Using Cs-137 and Am-241 sources resulted in energy resolutions for gamma-rays as good as 1-2% (FWHM) at room-temperature under non-optimized conditions.

\* corresponding author: e-mail: [uwe.hommerich@hamptonu.edu](mailto:uwe.hommerich@hamptonu.edu)

A2. Bridgman Technique, A1. Doping, B1. Halides, B1. Semiconducting material, B3. Infrared Devices

## 1. Introduction

Binary and ternary lead halide materials continue to be of current interest for possible applications as solid-state laser hosts [1-6], laser cooling materials [7,8], scintillators [9,10], and semiconductor nuclear radiation detectors [11,12]. For applications in solid-state lasers, most research has focused on ternary lead halide crystals of compositions  $APb_2X_5$  with  $A=K, Rb$  and  $X=Cl, Br$  [1-6]. Several IR laser demonstration were reported for rare earth doped  $KPb_2Cl_5$  and  $RbPb_2Cl_5$  operating at room temperature [6,13,14]. The low maximum phonon energies for ternary lead halides of  $\sim 200\text{ cm}^{-1}$  or smaller are of special importance for the development of long-wavelength IR lasers leading to greatly reduced non-radiative decay rates [15]. Among trivalent rare earth ions,  $Dy^{3+}$  is of great interest for IR laser applications due to several energy level separations of only  $\sim 1000\text{-}2500\text{ cm}^{-1}$  [15]. IR lasing from  $Dy^{3+}$  doped crystals and glasses has been demonstrated at various IR wavelengths (2.9, 4.4, 5.5  $\mu\text{m}$ ) using fluoride and chloride based laser hosts [6,16-18]. Besides applications in solid-state lasers, lead halide based crystals are also of current interest for nuclear radiation detection. For example, recent results of the wide-gap semiconductor  $CsPbBr_3$  have shown interesting properties for solid-state nuclear detection at room-temperature [19,20].

In this paper, we extended the work on ternary lead halides to  $TlPb_2Br_5$  (TPB), which has not yet been evaluated for laser applications or nuclear radiation detection. Results of the material preparation, purification studies, and bulk crystal growth are presented. The resulting crystals of undoped TPB and  $Dy: TPB$  were spectroscopically evaluated for potential applications in IR lasers and gamma-ray detection.

## 2. Material Properties, Purification, and Crystal Growth

TlPb<sub>2</sub>Br<sub>5</sub> crystallizes in a monoclinic NH<sub>4</sub>Pb<sub>2</sub>Cl<sub>5</sub>-type structure and belongs to the space group P2<sub>1</sub>/c. The lattice parameters are a=0.9304 nm, b=0.8336nm, c=1.3004nm [21]. The deviation of the monoclinic angle  $\beta$  from 90° is only very small. It has been reported that TPB melts congruently with a melting point at ~400 °C. The IR transparency range extends from ~0.40  $\mu$ m to 25 $\mu$ m [21]. The refractive index in the IR region was estimated from transmission data to be ~2.3 assuming that Fresnel reflections are the dominant cause for transmission losses [1]. This value is similar to the refractive index reported for Tl<sub>3</sub>PbBr<sub>5</sub> [22]. TlPb<sub>2</sub>Br<sub>5</sub> was synthesized from high purity and ultra-dry beads of PbBr<sub>2</sub> (99.999%) and TlBr (99.999%). The purchased materials were delivered in glass ampoules sealed under argon atmosphere. In order to prevent exposure to air, all handling of the purchased materials was carried out in an argon filled glove-box (oxygen<0.1ppm, H<sub>2</sub>O<0.1ppm). For initial purification, PbBr<sub>2</sub> and TlBr were separately loaded into pre-cleaned quartz ampoules and dried under vacuum for 2 days before sealing. After vacuum sealing, the loaded ampoules of both materials were molten in a two-zone vertical furnace and re-crystallized at speeds of 5-10 mm/hr. Following directional solidification, the middle parts of the resulting polycrystalline ingots of PbBr<sub>2</sub> and TlBr were used for the synthesis of TlPb<sub>2</sub>Br<sub>5</sub>. Stoichiometric proportions of PbBr<sub>2</sub> and TlBr were filled into a pre-cleaned quartz ampoule and further dried under a dynamic vacuum at a temperature of ~110 °C for ~ 24 hours. The loaded ampoule of the PbBr<sub>2</sub>-TlBr mixture was subsequently evacuated at a pressure of ~10<sup>-6</sup> Torr and vacuum sealed. The synthesis of ~80-100 g of TlPb<sub>2</sub>Br<sub>5</sub> was performed in a horizontal tube furnace at a temperature of ~450 °C followed by a multi-pass, uni-directional translation through a single zone-melting system. The temperature of the furnace was carefully adjusted to yield a molten zone of ~1-2 cm length. The translation speed ranged

from 5-10 mm/hr. After ~10 translations, the middle part of the ampoule contained clear and transparent pieces of high purity  $\text{TPb}_2\text{Br}_5$ , which were later used for doping and crystal growth experiments. For Dy doping, 2 wt.% of  $\text{DyBr}_3$  was added to the purified TPB material and vacuum-sealed ( $\sim 10^{-6}$  Torr) in a quartz ampoule. The material was molten in a horizontal tube furnace for a time period of two days for mixing. Crystal growth experiments of undoped TPB and Dy: TPB were performed in a two-zone tube furnace by a self-seeding Bridgman method. The crystal growth ampoules used had an inner diameter of 16 mm for TPB and 10.5 mm for Dy: TPB with cone-shaped ends. During the crystal growth process, the temperatures of the two zones were fixed at  $\sim 450$  °C and 350 °C, respectively. The vertical temperature gradient at the solid-melt interface was  $\sim 15$  °C/cm. The translation speed of the growth ampoule was held constant at  $\sim 3$  mm/hr. After the crystal growth was completed, the crystal was slowly cooled down to room-temperature over a time period of four days. The resulting undoped TPB and Dy:  $\text{TPb}_2\text{Br}_5$  ingots exhibited nearly crack-free sections of  $\sim 2$ -3 cm length. The undoped TPB crystal was clear with no coloration in the middle part of the ingot. The Dy: TPB crystal had a noticeable yellow color indicating the incorporation of  $\text{Dy}^{3+}$  ions in the host matrix. Figure 1 shows pictures of the as-grown crystals and samples prepared for spectroscopic studies.

### **3. Characterization Studies**

#### *3.1. Optical Transmission and Absorption*

For optical transmission studies of undoped TPB and Dy doped TPB,  $\sim 3$ -5 mm thick samples were cut from their corresponding ingots using a wire saw. The crystals were carefully polished to an optical finish using alumina polishing pad. The transmission spectra were recorded in the UV-VIS-NIR using a Shimadzu spectrophotometer and an FTIR spectrometer was employed for the longer IR region. The transmission spectra of undoped TPB and Dy: TPB

are shown in Figure 2. The undoped TPB sample showed a sharp absorption edge at  $\sim 400$  nm, corresponding to a bandgap energy of  $\sim 3.1$  eV. The IR transmission was as high as  $\sim 68\%$  with only weak structures in the  $2.8 \mu\text{m}$  region, which most likely arise due to some residual water absorption in the grown crystals. The Dy: TPB sample was of lower optical quality and exhibited an overall reduced transmission with a maximum value of less than  $47\%$ . In addition, the transmission revealed strong absorption bands at several visible and IR wavelengths indicating the incorporation of  $\text{Dy}^{3+}$  ions into the TPB host matrix. The background-corrected absorption spectrum is shown in the lower portion of Figure 2. The characteristic  $\text{Dy}^{3+}$  absorption bands originating from the  ${}^6\text{H}_{15/2}$  ground state are easily identified and relevant IR energy levels are indicated in the graph [15]. The strongest absorption band is located at  $\sim 1.3 \mu\text{m}$  ( ${}^6\text{H}_{15/2} \rightarrow {}^6\text{H}_{9/2} + {}^6\text{F}_{11/2}$  transition) and could be pumped using commercially available Nd:YAG lasers or diode lasers [X-new]. The Dy dopant concentration in the investigated sample was determined at Galbreith Laboratory using inductively coupled plasma optical emission spectroscopy (ICP-OES) to be  $3.3 \times 10^{20} \text{cm}^{-3}$ , which yields an absorption cross-section at  $1.3 \mu\text{m}$  of  $4.1 \times 10^{-20} \text{cm}^2$ .

### 3.2. Infrared Fluorescence Studies

The mid-IR emission from Dy: TPB in the  $\sim 2.5\text{-}4.5 \mu\text{m}$  region was excited using a  $\sim 1.36 \mu\text{m}$  diode-laser as the optical pump source. The emission was dispersed with a  $0.15 \text{ m}$  spectrometer (with grating turrets for  $2 \mu\text{m}$  and  $4 \mu\text{m}$ ) and the spectra were recorded using a lock-in amplifier. Figure 3 shows broad emission bands centered at  $2.8 \mu\text{m}$  and  $4.4 \mu\text{m}$  with a bandwidth FWHM of  $\sim 215 \text{ nm}$  and  $\sim 350 \text{ nm}$ , respectively. As indicated in the inset of Figure 3, the emissions can be assigned to the  $\text{Dy}^{3+}$  intra-4f transitions  ${}^6\text{H}_{13/2} \rightarrow {}^6\text{H}_{15/2}$  ( $2.8 \mu\text{m}$ ) and  ${}^6\text{H}_{11/2} \rightarrow {}^6\text{H}_{13/2}$  ( $4.3 \mu\text{m}$ ). The emission decay transients were found to be nearly single exponential with lifetime values of  $9.5 \text{ ms}$  for the  $2.8 \mu\text{m}$  band and  $\sim 5.2 \text{ ms}$  for the  $4.4 \mu\text{m}$  band. The long

emission lifetimes are consistent with reports for other Dy<sup>3+</sup> doped chloride and bromide crystals [1,6] and suggest that non-radiative decay through multi-phonon relaxations is negligibly small [15]. Using the well-known Ladenburg-Fuchtbauer relation [1,15], the peak emission cross-sections were determined to be  $\sim 0.8 \times 10^{-20} \text{ cm}^2$  and  $\sim 0.5 \times 10^{-20} \text{ cm}^2$ , respectively, which makes Dy: TPB a promising candidate for mid-IR laser applications.

### 3.3. Gamma-Ray detection experiments

Initial gamma-ray detection experiments were performed using an undoped TPB sample, which was cut and polished to a disk shape with  $\sim 2$  mm thickness. TlPb<sub>2</sub>Br<sub>5</sub> consists of elements with high atomic number (Tl: 81, Pb: 82; Br: 35) and has a high density of  $\sim 6.9 \text{ g}\cdot\text{cm}^{-3}$ , which indicates a short attenuation lengths for high energy photons. The large energy bandgap of  $\sim 3.1$  eV allows the possibility for TPB to operate as a room-temperature radiation detector without any cooling requirements. The resistivity was determined from I-V measurements to be as high as  $\sim 1.6 \times 10^{10} \Omega\cdot\text{cm}$ . For gamma-ray detection experiments, the signal was processed using a charge sensitive amplifier, a linear spectroscopy-shaping amplifier, and a multi-channel analyzer (MCA) interfaced with a computer. A pulser was used for electronic noise measurement along with data acquisition. Energy resolution as high as  $\sim 1\%$  was achieved using a 662 keV Cs-137 gamma ray source. A resolution of  $\sim 2\%$  was achieved using 59.6 keV gamma-rays from Am-241 (see Fig. 4). All of these results were obtained at room temperature without any additional signal processing correction. Further characterization studies and material optimization of TPB are currently being undertaken.

## 4. Conclusions

Results of the material synthesis, purification studies, and crystal growth of undoped TlPb<sub>2</sub>Br<sub>5</sub> and Dy-doped TlPb<sub>2</sub>Br<sub>5</sub> were presented. Nearly crack-free crystals with optical

transmissions as high as ~68% were obtained after careful purification of commercial starting materials. The undoped TPB crystal exhibited an absorption edge at ~3.1 eV and high resistivity of  $\sim 1.6 \times 10^{10} \Omega \cdot \text{cm}$ . Under exposure to gamma-rays from Cs-137 and Am-241 sources, energy spectra with resolutions as high as ~1-2% were observed at room-temperature, which makes TPB an interesting material for nuclear radiation detection. The investigated Dy-doped TPB crystal exhibited absorption bands characteristic for intra-4f transition of  $\text{Dy}^{3+}$  ions. Following optical pumping into the ~1.3  $\mu\text{m}$  absorption band, efficient IR emissions were observed centered at 2.8  $\mu\text{m}$  and 4.4  $\mu\text{m}$ . The combination of strong absorption bands, long emission lifetimes, and high emission cross-sections make Dy: TPB a promising candidate for mid-IR laser applications.

### **Acknowledgement**

The work at Hampton University was supported by the National Science Foundation through grants 1401077 and 1649150 and the Army Research Office through grant W911NF-16-1-0530.

## References

- [1] M. C. Nostrand, R. H. Page, S.A. Payne, L. I. Isaenko, and A. P. Yelisseyev, *J. Optical Society of America B* 18 (2001) 264.
- [2] N.W. Jenkins, S.R. Bowman, L. B. Shaw, J. R. Lindle, *J. Lumin.* 97 (2002) 127.
- [3] K. Rademaker, E. Heuman, G. Huber, S. A. Payne, W. F. Krupke, L. I. Isaenko, A. Burger, *Opt. Lett.* 30 (2005) 729.
- [4] A. Ferrier, M. Velazquez, J. L. Doualan, and R. J. Moncorge, *J. Appl. Phys.* 104 (2008) 23513.
- [5] U. Hömmerich, C. Hanley, E. Brown, S.B. Trivedi, and J. M. Zavada, *J. Alloys and Compd.* 488 (2009) 624.
- [6] A. G. Okhrimchuk, L. N. Butvina, E. M Dianov, I. A. Shestakova, N. V. Lichkova, V. N. Zagorodney, A. Shestakov, *J. Opt. Soc. Am. B* 24 (2007) 2690.
- [7] J. Fernandez, A. J. Garcia-Adeva, R. Balda, *Phys. Rev. Lett.* 97 (2006) 033001.
- [8] N. J. Condon, S. R. Bowman, S. P. O'Connor, R. S. Quimby, C. E. Mungan, *Opt. Express* 17 (2009) 5466.
- [9] M. Kobayashi, K. Omata, S. Sugimoto, Y. Tamagawa, T. Kuroiwa, H. Asada, H. Takeuchi, S. Kondo, *Nucl. Instr. Meth. A* 592 (2008) 369.
- [10] E. Rowe, E. Tupitsyn, P. Bhattacharya, L. Matei, M. Groza, V. Buliga, G. Atkinson, A. Burger, *J. Cryst. Growth* 393 (2014) 156.
- [11] J. C. Lund, K.S. Shah, M.R. Squillante, L.P. Moy, F. Sinclair, G. Entine, *Nucl. Instr. and Meth. A* 380 (1996) 169.
- [12] E.R. Manoel, M.C.C. Custodio, F.E.G. Guimaraes, R. F. Bianchi, A. C. Hernandez, *Mat. Res.*, 2 (1999) 75.
- [13] N. W. Jenkins, S. R. Bowman, S. O'Connor, S. K. Searles, J. Ganem, *Opt. Mater.* 22, (2003) 311-320.
- [14] N. Ter-Gabrielyan, T. Sanamyan, and M. Dubinskii, *Opt. Lett.* 34 (2009) 1949.
- [15] A. A. Kaminskii, *Crystalline lasers: Physical processes and operating schemes*, CRC press, New York (1996).
- [16] N. Djeu, V.E. Hartwell, A.A. Kaminskii, A. V. Butashin, *Opt. Lett.* 22 (1997) 997.
- [17] N. P. Barnes and R.E. Allen, *IEEE J. Quantum Electron.* 27 (1991) 277.
- [18] N.C. Nostrand, R.H. Page, S.A. Payne, W. F. Krupke, P.G. Schunemann, *Opt. Lett.* 24 (1999) 1215.
- [19] C.C. Stoumpos, C.D. Malliakas, J. A. Peters, Z. Lui, M. Sebastian, J. Im, T. C. Chasapis, A. C. Wibowo, D. Y. Chung, A. J. Feeman, B.C. Wessels, M. G. Kanatzidis, *Cryst. Growth Des.* 13 (2013) 2722.
- [20] D. N. Dirin, I. Chenukh, S. Yakunin, Y. Shynkarenko, M. V. Kovalenko, *Chem. Mater.* 2016, 28, 8470-8474.
- [21] O.Y. Khyzhun, V.L. Bekenev, N.M. Denysyuk, I.V. Kityk, P. Rakus, A.O. Fedorchuk, S. P. Danylchuk, O.V. Parasyuk, *Opt. Mater.* 36 (2013) 251.
- [22] A. Ferrier, M. Velazquez, R. Moncorge, *Phys. Rev. B* 77 (2008) 075122.
- [X] Y. H. Tsang, A. E. El-Taher, T. A. King, S. D. Jackson, "Efficient 2.96  $\mu\text{m}$  dysprosium-doped fluoride fiber laser pumped with a Nd: YAG laser operating at 1.3  $\mu\text{m}$ ", *Opt. Express* 14 (2006) 678.



**Figure captions:**

**Figure 1**

Pictures of as-grown crystals and polished samples of undoped  $\text{TlPb}_2\text{Br}_5$  (top) and Dy:  $\text{TlPb}_2\text{Br}_5$  (bottom).

**Figure 2**

Room-temperature transmission and absorption spectra of undoped  $\text{TlPb}_2\text{Br}_5$  (top) and Dy:  $\text{TlPb}_2\text{Br}_5$  (middle and bottom) crystals.

**Figure 3**

Room-temperature emission cross-section spectra and lifetimes of Dy: TPB for mid-IR bands centered at  $\sim 2.8 \mu\text{m}$  (top) and  $\sim 4.4 \mu\text{m}$  (bottom). The emission was excited using a  $1.36 \mu\text{m}$  diode laser. The inset shows a schematic diagram of the relevant lower energy levels of  $\text{Dy}^{3+}$  ions.

**Figure 4**

Cs-137 and Am-241 spectra collected with a  $\text{TlPb}_2\text{Br}_5$  sample ( $\sim 5 \times 5 \times 2 \text{mm}^3$ ) at room-temperature. An energy resolution of  $\sim 1\%$  (FWHM) at 662 keV and  $\sim 2\%$  (FWHM) at 59.6 keV was measured for  $\text{TlPb}_2\text{Br}_5$ .

Figure 1

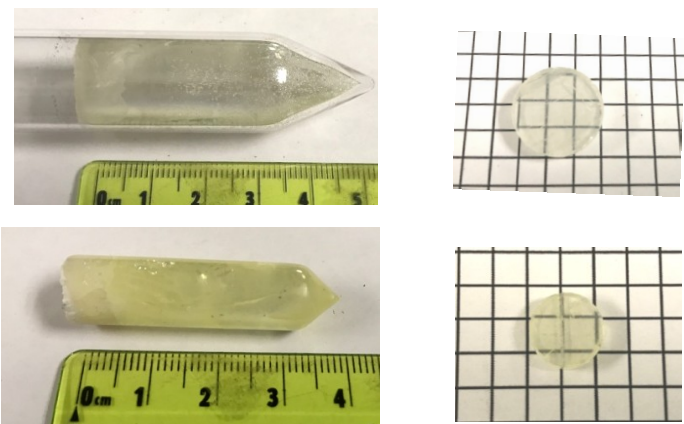


Figure 2

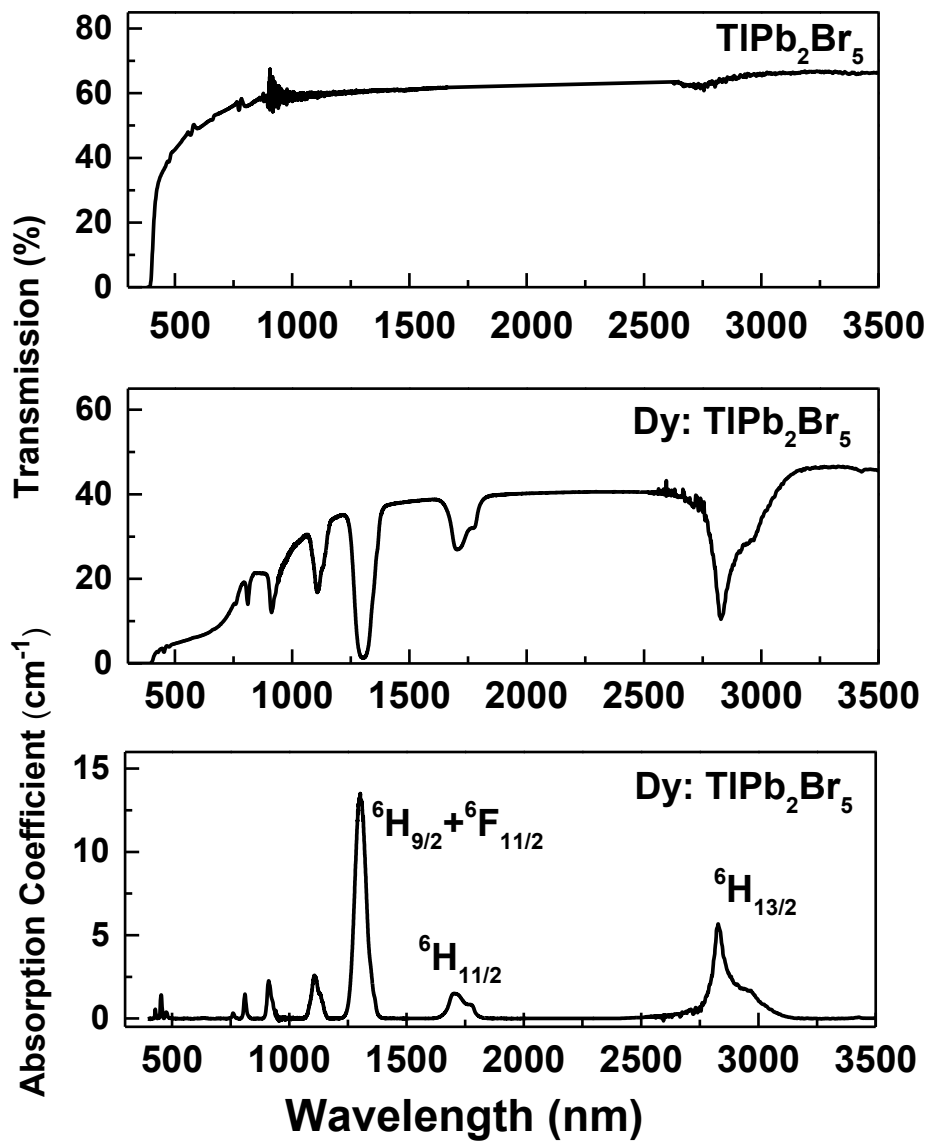


Figure 3

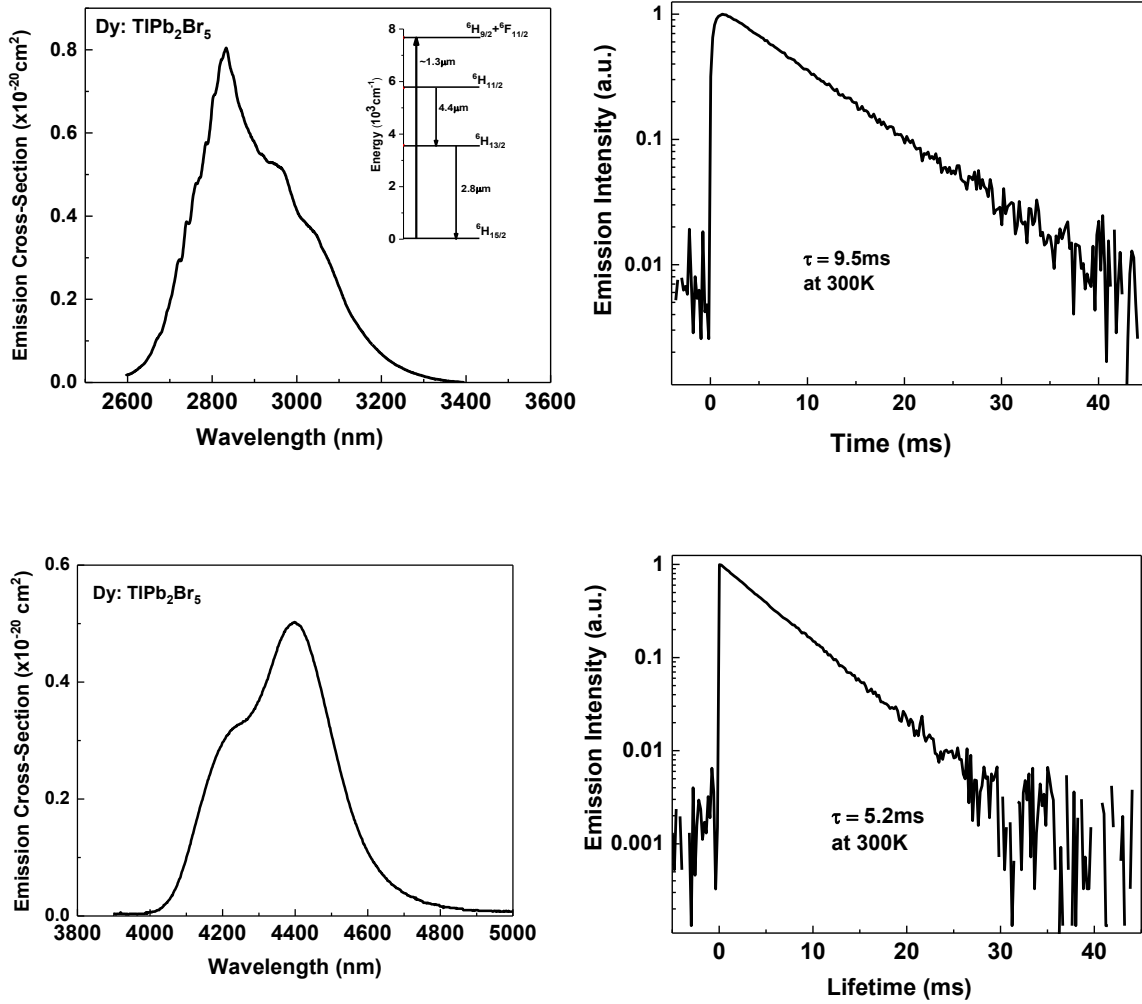


Figure 4

